# Optimizing Sectorized Wireless Networks: Model, Analysis, and Algorithm

Panagiotis Promponas†, Tingjun Chen‡, Leandros Tassiulas†

†Electrical Engineering, Yale University, ‡Electrical and Computer Engineering, Duke University

## ABSTRACT

Future wireless networks need to support the increasing demands for high data rates and improved coverage. One promising solution is sectorization, where an infrastructure node (e.g., a base station) is equipped with multiple sectors employing directional communication. Although the concept of sectorization is not new, it is critical to fully understand the potential of sectorized networks, such as the rate gain achieved when multiple sectors can be simultaneously activated. In this paper, we focus on sectorized wireless networks, where sectorized infrastructure nodes with beam-steering capabilities form a multi-hop mesh network for data forwarding and routing. We present a sectorized node model and characterize the capacity region of these sectorized networks. We define the flow extension ratio and the corresponding sectorization gain, which quantitatively measure the performance gain introduced by node sectorization as a function of the network flow. Our objective is to find the optimal sectorization of each node that achieves the maximum flow extension ratio, and thus the sectorization gain. Towards this goal, we formulate the corresponding optimization problem and develop an efficient distributed algorithm that obtains the node sectorization under a given network flow with an approximation ratio of 2/3. Through extensive simulations, we evaluate the sectorization gain and the performance of the proposed algorithm in various network scenarios with varying network flows. The simulation results show that the approximate sectorization gain increases sublinearly as a function of the number of sectors per node.

## CCS CONCEPTS

• **Networks** → **Network algorithms**; **Wireless access points, base stations and infrastructure**.

## KEYWORDS

Sectorized wireless networks, scheduling and routing, optimization

**ACM Reference Format:**

Panagiotis Promponas†, Tingjun Chen‡, Leandros Tassiulas†. 2023. Optimizing Sectorized Wireless Networks: Model, Analysis, and Algorithm. In *The Twenty-fourth International Symposium on Theory, Algorithmic Foundations, and Protocol Design for Mobile Networks and Mobile Computing (MobiHoc '23), October 23–26, 2023, Washington, DC, USA.* ACM, New York, NY, USA, 10 pages. https://doi.org/10.1145/3565287.3610272



*MobiHoc '23, October 23–26, 2023, Washington, DC, USA*



ACM ISBN 978-1-4503-9926-5/23/10.

https://doi.org/10.1145/3565287.3610272

## 1 INTRODUCTION

Future wireless networks and systems including 5G/6G need to provide multi-Gbps data rates with guaranteed coverage, leveraging massive antenna systems [22], the widely available spectrum at millimeter-wave (mmWave) frequency [18], and network densification [9]. In addition to deploying more cell cites, the *sectorization* of each cell – dividing each cell into a number of non-overlapping sectors – can significantly enhance the cell capacity and coverage by improving the spatial reuse and reducing interference [1].

There are many applications of sectorized networks to wireless access and backhaul networks, in both sub-6 GHz and mmWave frequency bands. For example, in a mmWave backhaul network that can provide fiber-like data rates (e.g., the Terragraph 60 GHz solution [13]), each mmWave node is usually composed of a number of sectors, each of which is equipped with a phased array with beamforming capability [20]. In addition, integrated access and backhaul (IAB) [16] in the mmWave band supporting flexible and sectorized multi-hop backhauling started to be standarized since 3GPP Release 16. Recent efforts also focused on using increased number of sectors per infrastructure node to provide better coverage (e.g., SuperCell [7] supports 36 azimuth sectors per node). Therefore, it is important to study the performance of sectorized networks, especially when each node can simultaneously activate multiple sectors for signal transmission and/or reception.

In this paper, we focus on the *modeling, analysis, and optimization of sectorized wireless networks*, where sectorized nodes form a multi-hop mesh network for data forwarding and routing. We consider the scenario where a sectorized infrastructure node can simultaneously activate many sectors supporting beam-steering capability, and focus on optimizing the sectorization of each node given the network conditions. We present the model of a sectorized wireless backhaul network consisting of (fixed) sectorized infrastructure nodes, and describe the link interference model and characterize the capacity region of these networks. For a sectorized network, we introduce a latent structure of its connectivity graph, called the auxiliary graph, which captures the underlying structural property of the network as a function of the sectorization of each node. We show that the capacity region of a sectorized network can be described by the matching polytope of its auxiliary graph.

Then, we present the definitions of *flow extension ratio* and the corresponding *sectorization gain* as a function of the network flow. These two metrics quantitatively measure how much the network flow can be extended in a sectorized wireless network, and thus quantifies the performance of the network sectorization. We formulate an optimization problem with the objective to find the optimal sectorization of the network that maximizes the flow extension ratio (i.e., achieves the highest sectorization gain) under a given network flow. Due to the analytical intractability of the problem,

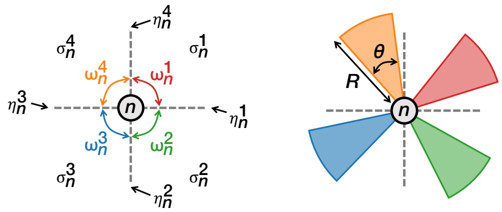
(a) (b)

**Figure 1: Sectorized infrastructure node model: (a) A sectorized node $n$ with $K_n = 4$ sectors, $\{\sigma_n^k\}$, the FoV of each sector, $\{\omega_n^k\}$, and the sectoring axes, $\{\eta_n^k\}$. (b) Each node sector can perform TX or RX beamforming with a range of $R$ and main lobe beamwidth of $\theta$.**

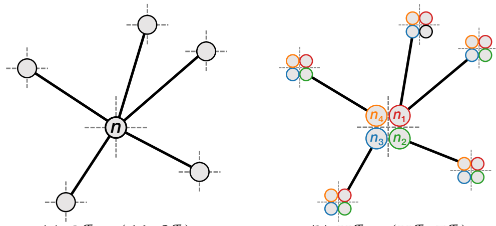
(a) $G^{\sigma} = (\mathcal{N}, \mathcal{L}^{\sigma})$ (b) $H^{\sigma} = (V^{\sigma}, E^{\sigma})$

**Figure 2: Graph representations of a sectorized network: (a) the connectivity graph of the physical network, $G^{\sigma} = (\mathcal{N}, \mathcal{L}^{\sigma})$, and (b) its corresponding auxiliary graph, $H^{\sigma} = (V^{\sigma}, E^{\sigma})$.**

we develop a novel distributed algorithm, Sectorize-$n$, that approximates the optimal sectorization of each node in the network. We also prove that Sectorize-$n$ is a 2/3-approximation algorithm.

Finally, we numerically evaluate the performance of the proposed algorithm through extensive simulations. We consider both an example 7-node network and a large number of random networks with varying numbers of sectors per node, node density, and network flows. The simulation results confirm our analysis and show that the approximate sectorization gain increases sublinearly with respect to the number of sectors per infrastructure node.

To summarize, the main contributions of this paper include:

(*i*) A general sectorized multi-hop wireless network model and a comprehensive characterization of its capacity region based on matching polytopes,

(*ii*) A distributed approximation algorithm that optimizes the sectorization of each node under a given network flow with performance guarantee, and

(*iii*) Extensive simulations for performance evaluation of the proposed sectorized network model and algorithm.

We also note that the developed sectorized network model and analysis are very general, and can be applied to other networks that share similar structures of the connectivity and auxiliary graphs.

## 2 RELATED WORK

There has been extensive work on characterizing the capacity region of sub-6 GHz wireless networks where each node is equipped with a single directional antenna (i.e., *without sectorization*), as well as on developing medium access control (MAC), scheduling, and routing algorithms for these directional networks [15, 24, 27]. Recently work also focused on mmWave networks where nodes apply beamforming techniques for directional communication, and considered multi-user MIMO and joint transmission [26], IAB [16], joint scheduling and congestion control [8], and the corresponding scheduling/routing and resource allocation problems in these networks. For networks *with sectorization*, recent work has considered the design of routing protocols when only a single sector can be activated at any time for each node (e.g., [19]).

Most relevant to our work are [2, 4, 10]. In particular, [4] focuses on efficient message broadcasting in multi-hop sectorized wireless networks, where each node has a pre-fixed sectorization. [10] considers the multi-hop link scheduling problem in self-backhauled mmWave cellular networks and applied deep reinforcement learning for minimizing the end-to-end delay. [2] considers the relay optimization problem between macro and micro base stations in mmWave backhaul networks with at most two-hop path lengths. In contrast, our work uniquely focuses on (*i*) characterizing the fundamental capacity of sectorized wireless networks when multiple sectors can be simultaneously activated at each node, (*ii*) optimizing the node sectorization in these networks under different network flow conditions, and (*iii*) analyzing the network-level gain introduced by optimizing the sectorization of each node, which has not been considered in prior work. To the best of our knowledge, this paper is *the first thorough study of these topics.*

## 3 MODEL AND PRELIMINARIES

### 3.1 Network Model

We consider a network consisting of $N$ *sectorized* infrastructure nodes. We denote the set of nodes by $\mathcal{N}$ and index them by $[n] = \{1, 2, \cdots, N\}$. In particular, let $\sigma_n$ denote the sectorization of node $n \in \mathcal{N}$ equipped with $K_n$ sectors. Let $\Gamma_n(K_n)$ denote the set of all possible sectorizations for node $n$ with a fixed number of $K_n$ sectors. As shown in Fig. 1(a), the $k^{\text{th}}$ sector of node $n$, denoted by $\sigma_n^k$ ($k = 1, \cdots, K_n$), has a field of view (FoV) of $\omega_n^k$, and the $K_n$ sectors of node $n$ combine to cover an FoV of the entire azimuth plane, i.e., $\sum_{k=1}^{K_n} \omega_n^k = 360°$. For two adjacent sectors $k$ and $(k+1)$ of node $n$ ($k = 1, \cdots, K-1$), we call their boundary *a sectoring axis* and denote it by $\eta_n^k$. We define the sectoring axis between sector $K$ and sector 1 with $\eta_n^K$. Let $\sigma = (\sigma_1, \cdots, \sigma_N) = [\sigma_n : \forall n \in \mathcal{N}]$ denote the *network sectorization*, and $\mathbf{K} = (K_1, \cdots, K_N) = [K_n : \forall n \in \mathcal{N}]$ be the vector of the number of sectors for all nodes. For a given $\mathbf{K} \in \mathbb{Z}_+^N$, let $\Gamma(\mathbf{K})$ be the set of all possible network sectorizations, where node $n$ is equipped with $K_n$ sectors.

Each sector of an infrastructure node is equipped with a half-duplex phased array antenna to perform transmit (TX) or receive (RX) beamforming. We adapt the sectored antenna model [3] to approximate the TX/RX beam pattern that can be formed by each sector, where $R$ is the TX/RX range and $\theta$ is the beamwidth of the main lobe, as depicted in Fig. 1(b). We assume that the beamwidth $\theta$ is smaller than the sector's FoV, and the TX/RX beam can be *steered* to be pointed in different directions within each sector.

We use a *directed* graph $G^{\sigma} = (\mathcal{N}, \mathcal{L})$ to denote the *connectivity graph* of the network under sectorization $\sigma \in \Gamma(\mathbf{K})$, where $\mathcal{N}$ (with $|\mathcal{N}| = N$) is the set of nodes and $\mathcal{L}$ (with $|\mathcal{L}| = L$) is the set of directed links. A directed link $\ell$ *from* node $n$ *to* node $n'$, denoted by $\ell = (n, n')$, exists if the distance between the two nodes is less than the sum of their communication range, i.e., $|\mathbf{x}(n) - \mathbf{x}(n')| \leq 2R$, where $\mathbf{x}(x)$ denotes the node's location vector (e.g., using the Cartesian coordinate system) and $|\cdot|$ denotes the $L_2$-norm. Without

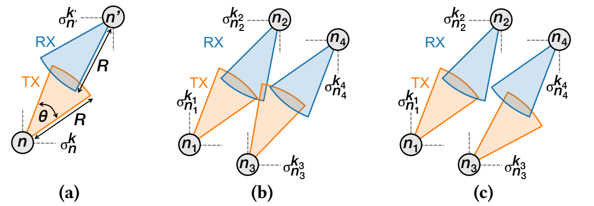


**Figure 3: (a) A feasible link $\ell = (\sigma_n^k, \sigma_{n'}^{k'})$, (b) A secondary interfering TX sector $\sigma_{n_3}^{k_3}$ to RX sector $\sigma_{n_2}^{k_2}$, (c) The secondary TX interference in (b) can be avoided by steering node 3's TX beam in $\sigma_{n_3}^{k_3}$, so that both links $(\sigma_{n_1}^{k_1}, \sigma_{n_2}^{k_2})$ and $(\sigma_{n_3}^{k_3}, \sigma_{n_4}^{k_4})$ can be simultaneously activated.**

loss of generality, we use $G$ (without the superscript $\sigma$) to denote the connectivity graph of an unsectorized network.

We also present an equivalent representation of each directed link in $G^\sigma$ based on the node sectors. In particular, each $\ell \in \mathcal{L}$ can also be represented by $\ell = (\sigma_n^k, \sigma_{n'}^{k'})$, where the $k^{\text{th}}$ sector of node $n$ (i.e., $\sigma_n^k$) is the *TX sector*, and the $k'^{\text{th}}$ sector of node $n'$ (i.e., $\sigma_{n'}^{k'}$) is the *RX sector*. For a link in the form of $(\sigma_n^k, \sigma_{n'}^{k'})$ to be a *feasible* link, it needs to satisfy the following two conditions[1] (see Fig. 3(a)):

- **(C1)** The distance between the two nodes is less than the sum of their communication range, i.e., $|\mathbf{x}(n) - \mathbf{x}(n')| \leq 2R$; and
- **(C2)** Node $n$ lies in the FoV $\omega_{n'}^{k'}$ of node $n'$, and node $n'$ lies in the FoV $\omega_n^k$ of node $n$.

Since both the TX and RX beams can be steered within $\omega_n^k$ of node $n$ and $\omega_{n'}^{k'}$ of node $n'$, respectively, the above two conditions are sufficient for establishing $\ell = (\sigma_n^k, \sigma_{n'}^{k'})$. Moreover, if $(\sigma_n^k, \sigma_{n'}^{k'})$ is a directional link, $(\sigma_{n'}^{k'}, \sigma_n^k)$ is also a directional link due to symmetry. Therefore, the set of feasible directed edges in $G^\sigma$ is given by:

$$\mathcal{L} = \big\{(n, n') : \forall n, n' \in \mathcal{N}, n \neq n', \text{ s.t. } (\mathbf{C1}) \text{ is satisfied}\big\}, \text{ or}$$

$$\mathcal{L}^\sigma = \big\{(\sigma_n^k, \sigma_{n'}^{k'}) : \forall n, n' \in \mathcal{N}, n \neq n', k \in [K_n], k' \in [K_{n'}], \text{ s.t. } (\mathbf{C1}) \text{ and } (\mathbf{C2}) \text{ are satisfied}\big\}.$$

Although $\mathcal{L}$ and $\mathcal{L}^\sigma$ are identical with respect to $G^\sigma$, for clarity, we use $\mathcal{L}^\sigma$ with superscript $\sigma$ to indicate the directed links represented by node sectors. Moreover, let $\mathcal{L}_n^+, \mathcal{L}_n^- \subseteq \mathcal{L}^\sigma$ denote the set of (directed) outgoing and incoming links with end point of node $n$.

**Remark.** Note that one of the main differences between the sectorized and traditional unsectorized networks is that *each node $n \in \mathcal{N}$ can have multiple links being activated at the same time, at most one per sector.* As a result, a number of links in $\mathcal{L}^\sigma$ can share the same end point (node) in $\mathcal{N}$ while being activated simultaneously. We use the terms "node" and "link" in reference to the *connectivity graph*, $G^\sigma$, while reserving the terms "vertex" and "edge" for the *auxiliary graph* of $G^\sigma$, which will be presented in §4.

## 3.2 Interference Model

The link interference model is essential for determining the set of directional links that can be activated simultaneously, or the *feasible schedules*. Our link interference model is based on the protocol model [11] adapted to the considered sectorized networks.

[1]A similar interference model was presented in [25], where beamforming can reduce the interference in mmWave networks. Our framework can also be generalized to other types of networks using their corresponding connectivity graphs.

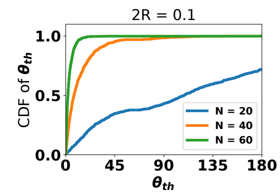


**Figure 4: The CDF of $\theta_{\text{th}}$ calculated for 1,000 random networks with $N \in \{20, 40, 60\}$ and a communication range of $2R = 0.1$.**

Definition 3.1 (Primary Interference Constraints in Sectorized Networks). *The transmission on a feasible link $(\sigma_n^k, \sigma_{n'}^{k'}) \in \mathcal{L}^\sigma$ from the $k^{th}$ sector of node $n$ to the $k'^{th}$ sector of node $n'$ is successful if it does not overlap with any other feasible directional link $(\sigma_n^k, \sigma_m^j)$ or $(\sigma_m^j, \sigma_{n'}^{k'})$ that share a TX or RX sector in common with $(\sigma_n^k, \sigma_{n'}^{k'})$. Essentially, at any time, at most one outgoing or incoming link is allowed in each node sector $\sigma_n^k, \forall n \in \mathcal{N}, k \in [K_n]$.*

Definition 3.2 (Secondary Interference Constraints in Sectorized Networks). *Consider two feasible directional links $\ell_{12} = (\sigma_{n_1}^{k_1}, \sigma_{n_2}^{k_2})$ and $\ell_{34} = (\sigma_{n_3}^{k_3}, \sigma_{n_4}^{k_4})$ between four distinct nodes $n_i$ ($i = 1, 2, 3, 4$) with fixed beamforming directions in each TX/RX sector. If the directional link $\ell_{32} = (\sigma_{n_3}^{k_3}, \sigma_{n_2}^{k_2})$ is also a feasible link and the TX beam in $\sigma_{n_3}^{k_3}$, which is intended to communicate with the RX beam in $\sigma_{n_4}^{k_4}$, overlaps with the RX beam in $\sigma_{n_2}^{k_2}$, then $\sigma_{n_3}^{k_3}$ is a secondary interfering TX sector to the RX sector $\sigma_{n_2}^{k_2}$ (see Fig. 3(b)).*

In this paper, we consider only primary interference constraints in sectorized networks, which is a realistic assumption because of two main reasons. First, note that secondary interference constraints can be avoided using the beam steering capacity of an infrastructure node. For the example depicted in Fig. 3(b), the interference from TX sector $\sigma_{n_3}^{k_3}$ to RX sector $\sigma_{n_2}^{k_2}$ can be avoided by steering the TX beam of node 3 in $\sigma_{n_3}^{k_3}$, so that both links $(\sigma_{n_1}^{k_1}, \sigma_{n_2}^{k_2})$ and $(\sigma_{n_3}^{k_3}, \sigma_{n_4}^{k_4})$ can be activated simultaneously, as shown in Fig. 3(c). Second, it is intuitive that for sufficiently small values of $\theta$, the network becomes highly directional with "pencil" beams. Essentially, there exists a threshold, $\theta_{\text{th}}$, below which the secondary interference constraints can be completely eliminated regardless of the TX/RX beamforming directions at each node. For each node $n$, let $\theta_n^{\min}$ denote the minimum angle between adjacent links with $n$ being an endpoint. Then, we have $\theta_{\text{th}} = \min_{n \in \mathcal{N}} \{\theta_n^{\min}\}$. In the example network shown in Fig. 6 (see §7.1 for the setup), $\theta_{\text{th}} = 15.8°$, which can be achieved by state-of-the-art phased arrays [20]. Fig. 4 illustrates the cumulative distribution function (CDF) of $\theta_{\text{th}}$ calculated over 1,000 random networks (see §7.2 for the setup) with $N \in \{20, 40, 60\}$ nodes deployed in a unit square area and when a communication range of $2R = 0.1$. The median value for $\theta_{\text{th}}$ is $107.0°/6.7°/2°$ for $N = 20/40/60$, respectively. This illustrates that in certain scenarios, it is reasonable to remove the secondary interference constraint under realistic node density and beamwidth.

## 3.3 Traffic Model, Schedule, and Queues

We assume that time is slotted and packets arrive at each node according to some stochastic process. For convenience, we classify all packets passing through the network to belong to a particular *commodity*, $c \in \mathcal{N}$, which represents the destination node of each packet. Let $A_n^{(c)}(t) \leq A_{\max} < +\infty$ be the number of commodity-$c$ packets entering the network at node $n$ and destined for node $c$ in slot $t$. The packet arrival process $A_n^{(c)}(t)$ is assumed to have a well-defined long-term rate of $\alpha_n^{(c)} = \lim_{T\to+\infty} \frac{1}{T}\sum_{t=1}^{T} A_n^{(c)}(t)$. Let $\boldsymbol{\alpha} = [\alpha_n^{(c)}]$ be the $N \times N$ multi-commodity arrival rate matrix.

All the (directional) links have a capacity of one packet per time slot. A *schedule* in any time slot $t$ is represented by a vector $\mathbf{X}(t) = [X_\ell(t)] \in \{0,1\}^L$, in which $X_\ell(t) = 1$ if link $\ell$ is scheduled to transmit a packet in time slot $t$ and $X_\ell(t) = 0$ otherwise. We denote the set of feasible schedules in $G^\sigma$ by $\mathcal{X}_{G^\sigma}$. In addition, let $\mu_\ell^{(c)}(t) = 1$ if link $\ell$ serves a commodity-$c$ packet in time $t$ (determined by the scheduling and routing algorithm), and $\mu_\ell^{(c)}(t) = 0$ otherwise. We define $Q_n^{(c)}(t)$ as the number of commodity-$c$ packets at node $n$ in time slot $t$, or the *queue backlog*. Choosing a schedule $\mathbf{X}(t) \in \mathcal{X}_{G^\sigma}$ and let $[x]^+ = \max\{0, x\}$, the queue dynamics are described by:

$$Q_n^{(c)}(t) = \left[Q_n^{(c)}(t-1) - \textstyle\sum_{\ell\in\mathcal{L}_n^+} X_\ell(t)\cdot\mu_\ell^{(c)}(t)\right]^+ + \textstyle\sum_{\ell\in\mathcal{L}_n^-} X_\ell(t)\cdot\mu_\ell^{(c)}(t) + A_n^{(c)}(t), \forall t.$$

We use $\mathbf{Q}(t) = [Q_n^{(c)}(t) : n, c \in \mathcal{N}]$ to denote the queue vector.

## 3.4 Capacity Region & Throughput Optimality

A dynamic scheduling and routing algorithm will determine the schedule $\mathbf{X}(t)$ in each time $t$. Let $f_\ell^{(c)}$ denote the long-term rate at which commodity-$c$ packets are served by link $\ell$, or the commodity-$c$ *flow* on link $\ell$. We define $\mathbf{f} = [f_\ell : \ell \in \mathcal{L}^\sigma]$ as the *network flow vector*, where $f_\ell = \sum_{c\in\mathcal{N}} f_\ell^{(c)}$ is the total flow served by link $\ell$.

The capacity region of the considered sectorized network $G^\sigma$, denoted by $\Lambda(G^\sigma)$, is defined as the set of all arrival rate matrices, $\boldsymbol{\alpha}$, for which there exists a multi-commodity network flow vector, $\mathbf{f}$, satisfying the flow conservation equations given by:

$$\alpha_{nc} = \sum_{\ell\in\mathcal{L}_c^+} f_\ell^{(c)} - \sum_{\ell\in\mathcal{L}_c^-} f_\ell^{(c)},\ \forall n \in \mathcal{N} \text{ and } n \neq c, \quad (1)$$

$$\sum_{n\in\mathcal{N}} \alpha_{nc} = \sum_{\ell\in\mathcal{L}_c^-} f_\ell^{(c)},\ \forall c \in \mathcal{N}, \quad (2)$$

$$f_\ell^{(c)} \geq 0,\ \forall \ell \in \mathcal{L}^\sigma, c \in \mathcal{N}, \quad (3)$$

$$f_\ell = \sum_{c\in\mathcal{N}} f_\ell^{(c)} \leq 1,\ \forall \ell \in \mathcal{L}^\sigma. \quad (4)$$

In particular, (1)–(3) define a *feasible* routing for commodity-$c$ packets, and (4) indicates that the total flow on each edge should not exceed its (unit) capacity. Therefore, for $G^\sigma = (\mathcal{N}, \mathcal{L}^\sigma)$, an arrival rate matrix $\boldsymbol{\alpha}$ is in the capacity region $\Lambda(G^\sigma)$ if there exists a *feasible* multi-commodity flow vector supporting $\boldsymbol{\alpha}$ with respect to the network defined by $G^\sigma$. As a result, we have

$$\Lambda(G^\sigma) = \left\{ \boldsymbol{\alpha} : \exists \mathbf{f} \in \mathrm{Co}(\mathcal{X}_{G^\sigma}) \text{ s.t. (1)–(4) are satisfied} \right\}, \quad (5)$$

where $\mathrm{Co}(\cdot)$ is the convex hull operator.

A scheduling and routing algorithm is called *throughput-optimal* if it can keep the network queues stable for all arrival rate matrices $\boldsymbol{\alpha} \in \mathrm{int}(\Lambda(G^\sigma))$, where $\mathrm{int}(\Lambda(G^\sigma))$ denotes the interior of $\Lambda(G^\sigma)$. A well-known throughput-optimal algorithm is the dynamic *backpressure routing algorithm* [23], which works as follows. For each link $\ell = (n, m) \in \mathcal{L}^\sigma$, we define its *backpressure* in time slot $t$ as $D_\ell(t) = \max_{c\in\mathcal{N}}\{Q_n^{(c)}(t) - Q_m^{(c)}(t)\}$. Let $\mathbf{D}(t) = [D_\ell(t) : \forall \ell \in \mathcal{L}^\sigma]$. In every time slot $t$, the backpressure algorithm selects $\mathbf{X}^{\mathrm{BP}}(t)$ as follows:

$$\mathbf{X}^{\mathrm{BP}}(t) \in \arg\max_{\mathbf{X}\in\mathcal{X}_{G^\sigma}} \{\mathbf{D}^\top(t)\cdot\mathbf{X}\}, \quad (6)$$

together with the commodity to be served on each link $\ell$. Given $\boldsymbol{\alpha} \in \mathrm{int}(\Lambda(G^\sigma))$, the backpressure algorithm returns a feasible network flow $\mathbf{f}$ that supports $\boldsymbol{\alpha}$ in $G^\sigma$. In the rest of the paper, although the target optimization problems may admit multiple optimal solutions, without loss of generality and for notational brevity, we treat them as singletons.

# 4 THE AUXILIARY GRAPH AND MATCHINGS

In this section, we introduce the auxiliary graph for a sectorized network, followed by an overview of matching polytopes and the definition of equivalent sectorizations. All of these serve as the foundations for the results presented in the remaining of this paper.

## 4.1 The Auxiliary Graph, $H^\sigma$

To allow for analytical tractability and support the analysis, we introduce the *auxiliary graph*, $H^\sigma = (V^\sigma, E^\sigma)$ of the considered sectorized network, under a given sectorization rule, $\sigma \in \Gamma(\mathbf{K})$. In particular, $H^\sigma$ is generated based on the connectivity graph $G^\sigma = (\mathcal{N}, \mathcal{L}^\sigma)$ as follows:

- Each node $n \in V$ is duplicated $K_n$ times into a set of *vertices*, $\{n_1, \cdots, n_{K_n}\} \in V^\sigma$, one for each node sector $\sigma_n^k,\ k \in [K_n]$.
- Each directed link $\ell = (\sigma_n^k, \sigma_{n'}^{k'}) \in \mathcal{L}^\sigma$ between the TX sector $\sigma_n^k$ and RX sector $\sigma_{n'}^{k'}$ is "inherited" as a directed *edge* $e$ from vertex $n_k$ to vertex $n'_{k'}$ in $V^\sigma$.

It is easy to see that $|V^\sigma| = \sum_{n\in\mathcal{N}} K_n$ and $|E^\sigma| = |\mathcal{L}| = L$, and as we show in the rest of the paper, $H^\sigma$ can largely facilitate the analysis and optimization in sectorized networks. An illustrative example is shown in Fig. 2, where each node in $G^\sigma$ has an equal number of 4 sectors based on the Cartesian coordinate system. Specifically, node $n$ in $G^\sigma$ is duplicated 4 times to become $n_i$ ($i = 1, 2, 3, 4$) in $H^\sigma$, while the 5 feasible links in $\mathcal{L}^\sigma$ are "inherited" from $G^\sigma$ to $H^\sigma$, whose end points are the duplicated vertices representing the corresponding TX/RX sectors.

## 4.2 Feasible Schedules in $G^\sigma$ as Matchings in $H^\sigma$

For an unsectorized network $G$ (i.e., $\sigma = \emptyset$) with $K_n = 1, \forall n$, its auxiliary graph $H = (V, E)$ is identical to the connectivity graph $G = (\mathcal{N}, \mathcal{L})$. Therefore, we use $G$ and $H$ interchangeably when referring to an unsectorized network. Each feasible schedule $\mathbf{X} \in \mathcal{X}_G$ is a *matching* – a set of links among which no two links share a common node – in $G$ (and thus in $H$).

However, in a sectorized network $G^\sigma = (\mathcal{N}, \mathcal{L}^\sigma)$, a feasible schedule in $G^\sigma$ may not be a matching in $G^\sigma$, since up to $K_n$ links can share a common node $n$. However, it is easy to see that under the primary interference constraints and with the use of the auxiliary graph, *any* feasible schedule in $G^\sigma$ corresponds to a matching in $H^\sigma$. Let $\mathbf{M} \in \{0,1\}^L$ denote a matching vector in $H^\sigma$, in which every element (edge) is ordered according to the position of the element (link) that it corresponds to in $\mathbf{X}$. Let $\mathcal{M}_{H^\sigma}$ be the set of matchings in $H^\sigma$. To rigorously connect a feasible schedule $\mathbf{X} \in \mathcal{X}_{G^\sigma}$ in $G^\sigma$ to a matching $\mathbf{M} \in \mathcal{M}_{H^\sigma}$ in $H^\sigma$, we need to take a deeper look into the sets $\mathcal{L}^\sigma$ and $E^\sigma$: they not only have the same cardinality of $L$, but are also in fact two *isomorphic* sets. In particular, due to the way $H^\sigma$ is constructed, there exists an isomorphism $O : E^\sigma \to \mathcal{L}^\sigma$ such that for $e = (n_k, n'_{k'}) \in E^\sigma$ and $\ell = (\sigma_n^k, \sigma_{n'}^{k'}) \in \mathcal{L}^\sigma$, $O(e) = \ell$.

## 4.3 Background on Matching Polytopes

The *matching polytope* of a (general) graph $G = (V, E)$, denoted by $\mathcal{P}_G$, is a convex polytope whose corners correspond to the matchings in $G$, and can be described using Edmonds' matching polytope theorem [5]. Specifically, a vector $\mathbf{x} = [x_e : e \in E] \in \mathbb{R}^{|E|}$ belongs to $\mathcal{P}_G$ if and only if it satisfies the following conditions [5, 14]:

$$\textbf{(P)} \quad (i) \quad x_e \geq 0,\ \forall e \in E, \text{ and } \textstyle\sum_{e \in \delta(n)} x_e \leq 1,\ \forall v \in V,$$

$$(ii) \quad \textstyle\sum_{e \in E(U)} x_e \leq \lfloor |U|/2 \rfloor,\ \forall U \subseteq V \text{ with } |U| \text{ odd}, \qquad (7)$$

where $\delta(v)$ is the set of edges incident to $v$, and $E(U)$ is the set of edges in the subgraph induced by $U \subseteq G$. Note that in general, it is challenging to compute $\mathcal{P}_G$, since (*ii*) of (7) includes an exponential number of constraints since all sets of vertices $U \subseteq V$ with an odd cardinality need to be enumerated through. The *fractional matching polytope* of $G$, denoted by $\mathcal{Q}_G$, is given by

$$\textbf{(Q)} \quad x_e \geq 0,\ \forall e \in E, \text{ and } \textstyle\sum_{e \in \delta(n)} x_e \leq 1,\ \forall v \in V. \qquad (8)$$

For a general graph $G$, $\mathcal{P}_G \subseteq \mathcal{Q}_G$ since (*ii*) in (**P**) is excluded in (**Q**). For a bipartite graph $G_{bi}$[2], its matching polytope and fractional matching polytope are equivalent, i.e., $\mathcal{P}_{G_{bi}} = \mathcal{Q}_{G_{bi}}$ [21].

Recall that for an unsectorized network $G$, its auxiliary graph $H \equiv G$ and its matching polytope is the convex hull of the set of matchings, i.e., $\mathcal{P}_H = \mathrm{Co}(\mathcal{M}_H)$. Therefore, its capacity region $\Lambda(G)$ is determined by $\mathcal{P}_H$, since $\mathcal{X}_G = \mathcal{M}_H$. For a sectorized network $G^\sigma$, since a feasible schedule in $G^\sigma$, $\mathbf{X} \in \mathcal{X}_{G^\sigma}$, corresponds to a matching in the auxiliary graph $H^\sigma$, $\mathbf{M} \in \mathcal{M}_{H^\sigma}$ (see §4.2), we show in §5 that its capacity region, $\Lambda(G^\sigma)$, can be determined by the matching polytope of $H^\sigma$, $\mathcal{P}_{H^\sigma}$ (Lemma 5.1).

## 4.4 Equivalent Sectorizations

Since our objective is to obtain the optimal sectorization for each node in the network, it is important to understand the structural property of a sectorization, $\sigma$. In particular, for a node $n \in \mathcal{N}$ with $K_n$ number of sectors, there is only *a finite number of distinct sectorizations* in $\Gamma_n(K_n)$, due to the equivalent classes of sectorizations.

Consider a node $n \in \mathcal{N}$ and two of its undirected adjacent incident links $\ell_1 = (n, u)$ and $\ell_2 = (n, v)$ for some $u, v$ incident to $n$. To define the undirected links from the set $\mathcal{L}$, we assume, for example, that the undirected link $\ell_1$ includes the two directed links $(n, u) \in \mathcal{L}_n^+$ and $(u, n) \in \mathcal{L}_n^-$. Note that, under the primary interference constraints, it does not make a difference where exactly a sectorization axis is put between $\ell_1$ and $\ell_2$ of node $n$. Instead, what matters is whether a sectorization axis will be placed between them or not. If two sectorizations $\sigma_1 \in \Gamma_n(K_n)$ and $\sigma_2 \in \Gamma_n(K_n)$ differ only on the exact position of a sectorization axis while both sectorization have a sectoring axis placed between $\ell_1$ and $\ell_2$, it holds that $H^{\sigma_1} \equiv H^{\sigma_2}$, and thus $\mathcal{M}_{H^{\sigma_1}} = \mathcal{M}_{H^{\sigma_2}}$. Therefore, the set $\Gamma_n(K_n)$ consists of a finite number of equivalent sectorizations.

Fig. 5 depicts an example of three equivalent sectorizations for node $n$, where both links $\ell_1 = (n, u)$ and $\ell_2 = (n, v)$ are placed within the same sector. Note that this notion of equivalent sectorizations

[2] A bipartite graph is a graph whose vertices can be divided into two *disjoint* and *independent* sets $U_1$ and $U_2$ such that every edge connects a vertex in $U_1$ to one in $U_2$.

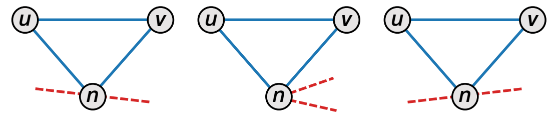


**Figure 5: Three equivalent sectorizations for a node $n \in \mathcal{N}$.**

makes the optimization over the set $\Gamma(\mathbf{K})$, for every fixed $\mathbf{K} \in \mathbb{Z}_+^N$, more approachable. Motivated by the comparison of sectorizations of Fig. 5, when rotating a sectorization axis of node $n$, an infinite number of equivalent sectorizations can be generated until the axis meets the next incident link. Therefore, up to an equivalence relation, the sectorization of a network, $\sigma \in \Gamma(\mathbf{K})$ is determined by whether a sectoring axis will be placed (instead of where exactly it will be placed) between adjacent undirected links of each node.

For node $n$, since a sectoring axis cannot be placed between the outgoing and incoming links corresponding to the same neighboring node of $n$, we consider undirected links regarding node $n$'s sectorization, $\sigma_n$. In the rest of the paper, let $\delta(n)$ denote the set of the undirected incident links of $n$, i.e., $\delta(n) = \{\ell_1, \cdots, \ell_{|\delta(n)|}\}$, ordered in a way such that geometrically neighboring (consecutive) undirected links are next to each other. Note that $\ell_{|\delta(w)|}$ and $\ell_1$ are also adjacent links due to the cyclic nature of $\sigma_n$. Using this notation, the sectorization of node $n$, $\sigma_n \in \Gamma_n(K_n)$, essentially partitions $\delta(n)$ into $K_n$ non-overlapping subsets of links. We can also denote $\sigma_n$ by placing the symbol "|" between two adjacent links where a sectoring axis is placed (e.g., $\delta_n = \{|(n, u), (n, v)\}$ in Fig. 5).

# 5 SECTORIZATION GAIN BASED ON NETWORK FLOW EXTENSION RATIO

In this section, we characterize the capacity region of sectorized networks and present the definitions of flow extension ratio and the corresponding sectorization gain. We consider a *general* sectorized network $G^\sigma$ under sectorization $\sigma \in \Gamma(\mathbf{K})$ with given $\mathbf{K} \in \mathbb{Z}_+^N$, and its auxiliary graph $H^\sigma$. Let $\mathcal{P}_{H^\sigma}$ be the matching polytope of $H^\sigma$.

We first present the following lemma that relates the convex hull of all feasible schedules in $G^\sigma$ to $\mathcal{P}_{H^\sigma}$ (for detailed proof see [17]).

LEMMA 5.1. *For a sectorized network $G^\sigma$ and its auxiliary graph $H^\sigma$, let $\mathcal{X}_{G^\sigma}$ be the set of feasible schedules in $G^\sigma$ and $\mathcal{M}_{H^\sigma}$ be the set of matchings in $H^\sigma$. Under the primary interference constraints, it holds that $\mathcal{X}_{G^\sigma} = \mathcal{M}_{H^\sigma}$ and $\mathrm{Co}(\mathcal{X}_{G^\sigma}) = \mathrm{Co}(\mathcal{M}_{H^\sigma}) = \mathcal{P}_{H^\sigma}$.*

Based on Lemma 5.1, the backpressure algorithm that obtains *maximum weight schedule (MWS)* $\mathbf{X}^{\mathrm{BP}}(t)$ in $G^\sigma$ (see §3.4), which in general is NP-hard, is equivalent to finding the corresponding *maximum weight matching (MWM)* in $H^\sigma$, with the backpressure $\mathbf{D}(t)$ being the weights on the edges, i.e.,

$$\mathbf{X}^{\mathrm{BP}}(t) := \arg\max_{\mathbf{X} \in \mathcal{X}_{G^\sigma}} \left\{\mathbf{D}^\top(t) \cdot \mathbf{X}\right\} = \arg\max_{\mathbf{M} \in \mathcal{M}_{H^\sigma}} \left\{\mathbf{D}^\top(t) \cdot \mathbf{M}\right\}.$$

From Edmond's theory [6, 21], the MWM of $H^\sigma$ can be obtained via a polynomial-time algorithm with complexity of $O(|V^\sigma|^2 \cdot |E|)$.

Intuitively, it is expected that $G^\sigma$ under sectorization $\sigma$ (with $H^\sigma = (V^\sigma, E^\sigma)$) has a capacity region that is at least the same as the unsectorized network $G$ (with $H = (V, E)$), i.e., any network flow $\mathbf{f}$ that can be maintained in the unsectorized network $G$ can always be maintained in $G^\sigma$. This is by the following theorem, whose proof can be found in [17].

THEOREM 5.2. $\mathcal{P}_G = \mathcal{P}_H \subseteq \mathcal{P}_{H^\sigma}$, $\forall \mathbf{K} \in \mathbb{Z}_+^N$ *and* $\forall \sigma \in \Gamma(\mathbf{K})$.

Based on (5) and Lemma 5.1, the capacity region of a sectorized network $G^\sigma$ can be characterized by the matching polytope of its auxiliary graph, $\mathcal{P}_{H^\sigma}$. With a given (unknown) $\boldsymbol{\alpha} \in \text{int}(\Lambda(G^\sigma))$ and a sectorization $\sigma$, the dynamic backpressure algorithm will converge to and return a network flow vector $\mathbf{f} \in \mathcal{P}_{H^\sigma}$. We define the flow extension ratio, denoted by $\lambda^\sigma(\mathbf{f})$, which quantitatively measures *how much the network flow* $\mathbf{f}$ *can be extended in its direction until it intersects the boundary of* $\mathcal{P}_{H^\sigma}$.

DEFINITION 5.3 (FLOW EXTENSION RATIO). *For a sectorized network* $G^\sigma$ *and network flow* $\mathbf{f} \in \mathcal{P}_{H^\sigma}$, *the flow extension ratio,* $\lambda^\sigma(\mathbf{f})$, *is the maximum scalar such that* $\lambda^\sigma(\mathbf{f}) \cdot \mathbf{f} \in \mathcal{P}_{H^\sigma}$ *still holds.*

Let $\zeta^\sigma(\mathbf{f}) := \min_{U \subseteq V^\sigma, |U| \text{ odd}} \left( \frac{\lfloor |U|/2 \rfloor}{\sum_{e \in E(U)} f_e} \right)$ (see (7)). With a little abuse of notation, for node $n$, network flow $\mathbf{f}$, and an undirected edge $e \in \delta(n)$ with directed components $e_+ \in \mathcal{L}_n^+$ and $e_- \in \mathcal{L}_n^-$, we let $f_e = f_{e_+} + f_{e_-}$. The flow extension ratio, $\lambda^\sigma(\mathbf{f})$, can be obtained by the following optimization problem:

$$\lambda^\sigma(\mathbf{f}) := \max_{\lambda \in \mathbb{R}^+} \lambda, \text{ s.t.: } \lambda \cdot \mathbf{f} \in \mathcal{P}_{H^\sigma}$$
$$\overset{(7)}{=} \min\Big\{ \min_{v \in V^\sigma} \frac{1}{\sum_{e \in \delta(v)} f_e}, \zeta^\sigma(\mathbf{f}) \Big\}. \quad (9)$$

Similarly, we define the flow extension ratio for the corresponding unsectorized network $G$, denoted by $\lambda^\varnothing(\mathbf{f}) := \max_{\lambda \in \mathbb{R}^+} \lambda$, s.t.: $\lambda \cdot \mathbf{f} \in \mathcal{P}_G$. Note that $\lambda^\varnothing(\mathbf{f})$ depends solely on the topology of $G$ and is independent of the sectorization $\sigma$. Next, we define the *approximate flow extension ratio* with respect to the polytope $\mathcal{Q}_{H^\sigma}$.

DEFINITION 5.4 (APPROXIMATE FLOW EXTENSION RATIO). *For a sectorized network* $G^\sigma$ *and a network flow* $\mathbf{f} \in \mathcal{P}_{H^\sigma}$, *the approximate flow extension ratio,* $\mu^\sigma(\mathbf{f})$, *is the maximum scalar such that* $\mu^\sigma(\mathbf{f}) \cdot \mathbf{f} \in \mathcal{Q}_{H^\sigma}$ *still holds.*

The following optimization problem determines $\mu^\sigma(\mathbf{f})$:

$$\mu^\sigma(\mathbf{f}) := \max_{\mu \in \mathbb{R}^+} \mu, \text{ s.t.: } \mu \cdot \mathbf{f} \in \mathcal{Q}_{H^\sigma}$$
$$\overset{(8)}{=} \min_{v \in V^\sigma} \frac{1}{\sum_{e \in \delta(v)} f_e} = \frac{1}{\max_{v \in V^\sigma} \sum_{e \in \delta(v)} f_e}, \quad (10)$$

We also define the approximate flow extension ratio for the unsectorized network $G$, denoted by $\mu^\varnothing(\mathbf{f}) := \max_{\lambda \in \mathbb{R}^+} \lambda$, s.t.: $\lambda \cdot \mathbf{f} \in \mathcal{Q}_G$.

To quantitatively evaluate the performance of a sectorization $\sigma$, we present the following definition of sectorization gains.

DEFINITION 5.5 (SECTORIZATION GAINS). *The (explicit) sectorization gain of* $\sigma$ *with a network flow* $\mathbf{f}$ *is defined as* $g_\lambda^\sigma(\mathbf{f}) := \frac{\lambda^\sigma(\mathbf{f})}{\lambda^\varnothing(\mathbf{f})}$ *(with respect to* $\mathcal{P}_{H^\sigma}$*). The approximate sectorization gain of* $\sigma$ *with a network flow* $\mathbf{f}$ *is defined as* $g_\mu^\sigma(\mathbf{f}) := \frac{\mu^\sigma(\mathbf{f})}{\mu^\varnothing(\mathbf{f})}$ *(with respect to* $\mathcal{Q}_{H^\sigma}$*).*

The following lemma states the relationships between $\lambda^\sigma(\mathbf{f})$ and $\mu^\sigma(\mathbf{f})$, and between $g_\lambda^\sigma(\mathbf{f})$ and $g_\mu^\sigma(\mathbf{f})$, whose proof is in [17].

LEMMA 5.3. *For any sectorization* $\sigma$ *and network flow* $\mathbf{f}$, *it holds that: (i)* $\frac{2}{3} \cdot \mu^\sigma(\mathbf{f}) \leq \lambda^\sigma(\mathbf{f}) \leq \mu^\sigma(\mathbf{f})$, *(ii)* $\frac{1}{\mu^\sigma(\mathbf{f})} \geq \frac{1}{\lambda^\sigma(\mathbf{f})} - \max_{e \in E^\sigma} f_e$, *and (iii)* $\frac{2}{3} \cdot g_\mu^\sigma(\mathbf{f}) \leq g_\lambda^\sigma(\mathbf{f}) \leq \frac{3}{2} \cdot g_\mu^\sigma(\mathbf{f})$.

# 6 OPTIMIZATION AND A DISTRIBUTED APPROXIMATION ALGORITHM

Given a vector $\mathbf{K} \in \mathbb{Z}_+^N$, our objective is to find the sectorization $\sigma \in \Gamma(\mathbf{K})$ that maximizes the flow extension ratio, $\lambda^\sigma(\mathbf{f})$, under a network flow, $\mathbf{f}$. This optimization problem, (**Opt**), is given by:

$$(\textbf{Opt})\ \sigma^\star(\mathbf{f}) := \arg\max_{\sigma \in \Gamma(\mathbf{K})} \lambda^\sigma(\mathbf{f})$$
$$\overset{(9)}{=} \arg\max_{\sigma \in \Gamma(\mathbf{K})} \Big\{ \min\Big\{ \min_{v \in V^\sigma} \frac{1}{\sum_{e \in \delta(n)} f_e}, \zeta^\sigma(\mathbf{f}) \Big\}\Big\}. \quad (11)$$

Note that we are optimizing towards the boundary of the matching polytope, $\mathcal{P}_{H^\sigma}$, over the set of sectorizations, $\Gamma(\mathbf{K})$, for a given network flow, $\mathbf{f}$. This is because in general, there does not exist a single sectorization $\sigma \in \Gamma(\mathbf{K})$ that can achieve close-to-optimal performance of $\lambda^\sigma(\mathbf{f})$ for every network flow $\mathbf{f} \in \mathbb{R}^{|E|}$.

## 6.1 Key Insight and Intuition

In general, (**Opt**) is analytically intractable due to its combinatorial nature and the fact that $\zeta^\sigma(\mathbf{f})$ needs exponentially many calculations even for a fixed sectorization $\sigma$. Instead, we consider an alternative optimization problem:

$$(\textbf{Opt-Approx})\ \widetilde{\sigma}(\mathbf{f}) := \arg\max_{\sigma \in \Gamma(\mathbf{K})} \mu^\sigma(\mathbf{f})$$
$$\overset{(10)}{=} \arg\max_{\sigma \in \Gamma(\mathbf{K})} \Big\{ \min_{v \in V^\sigma} \frac{1}{\sum_{e \in \delta(v)} f_e} \Big\}. \quad (12)$$

Although (**Opt-Approx**) excludes the constraint $\zeta^\sigma(\mathbf{f})$ in (**Opt**), solving it by a brute-force algorithm is still analytically intractable due to the coupling between the (possibly different) sectorization of *all* nodes. For example, if each of the $N$ nodes has a number of $\widetilde{K}$ possible sectorizations, a total number of $N^{\widetilde{K}}$ sectorizations need to be evaluated in order to solve (**Opt-Approx**).

Our key insight behind developing a distributed approximation algorithm (described in §6.2) is that (**Opt-Approx**) can be decomposed into $N$ individual optimization problems, (**Opt-Approx**-$n$), for each node $n \in \mathcal{N}$. With a little abuse of notation, let $\mathbf{f}_n = (f_e : e \in \delta(n))$ be the "local" flows on the undirected edges incident to node $n$. This decomposed optimization problem is given by:

$$(\textbf{Opt-Approx-}n)\ \nu_n(\mathbf{f}_n) := \arg\min_{\sigma_n \in \Gamma_n(K_n)} \max_{v \in \{n_1^{\sigma_n}, \cdots, n_{K_n}^{\sigma_n}\}} \sum_{e \in \delta(v)} f_e. \quad (13)$$

(**Opt-Approx**-$n$) determines the sectorization of node $n$, $\nu_n(\mathbf{f}_n)$, based on its local flows, $\mathbf{f}_n$, and is *independent* of the other nodes. The following lemma shows that the sectorization obtained by solving the $N$ decomposed problems, (**Opt-Approx**-$n$), is equivalent to that obtained by solving (**Opt-Approx**), whose proof is in [17].

LEMMA 6.4. *For a given network flow* $\mathbf{f}$, *the sectorization* $\nu(\mathbf{f})$, *which consists of the solutions of (**Opt-Approx**-n) for all nodes* $n \in \mathcal{N}$, *is equivalent to the solution* $\widetilde{\sigma}(\mathbf{f})$ *to (**Opt-Approx**), i.e.,*

$$\widetilde{\sigma}(\mathbf{f}) = \nu(\mathbf{f}) = (\nu_1(\mathbf{f}_1), \cdots, \nu_N(\mathbf{f}_N)) \text{ and } \mu^\nu(\mathbf{f}) = \mu^{\widetilde{\sigma}}(\mathbf{f}). \quad (14)$$

Although (**Opt-Approx**-$n$) is a distributed optimization problem for each node $n$, to solve it using a brute-force method still remains high complexity. Consider the sectorization of node $n$ with $|\delta(n)|$ incident edges into $K_n$ sectors ($|\delta(n)| \leq (N-1)$). To solve (**Opt-Approx**-$n$) in a brute-force way, a total number of

**Algorithm 1** SECTORIZE-$n$ for node $n$.

**Input**: $K_n$, $\delta(n)$, $\mathbf{f}_n$, and $\epsilon$
$T_{\min} \leftarrow \max_{e\in\delta(n)} f_e$, $T_{\max} \leftarrow \sum_{e\in\delta(n)} f_e$, $T_{\text{temp}} \leftarrow 0$
$T_n^{\text{crit}} \leftarrow 0$, decision $\leftarrow$ No
**while** $(T_{\max} - T_{\min}) > \epsilon$ **do**
  $T_{\text{temp}} \leftarrow (T_{\min} + T_{\max})/2$
  (decision, $\pi_0$) $\leftarrow$ EXISTSECTORIZATION-$n(T_{\text{temp}})$ (Algorithm 2)
  **if** decision = Yes **then**
    $T_{\max} \leftarrow T_{\text{temp}}$
  **else**
    $T_{\min} \leftarrow T_{\text{temp}}$
  **end if**
**end while**
$T_n^{\text{crit}} \leftarrow T_{\max}$
(decision, $\pi_n(\mathbf{f}_n)$) $\leftarrow$ EXISTSECTORIZATION-$n(T_n^{\text{crit}})$
**return** The sectorization for node $n$, $\pi_n(\mathbf{f}_n)$

$\binom{|\delta(n)|}{K_n} = O\binom{N}{K_n} = O(N^{K_n})$ possible sectorizations need to be enumerated. Next, we present a polynomial-time distributed algorithm that solves (**Opt-Approx**-$n$) with a complexity independent of $K_n$.

## 6.2 A Distributed Approximation Algorithm

We now present *a distributed approximation algorithm*, SECTORIZE-$n$, that efficiently solves (**Opt**) with guaranteed performance. In essence, SECTORIZE-$n$ solves (**Opt-Approx**-$n$) for each individual node $n \in \mathcal{N}$. Algorithm 1 presents the pseudocode for SECTORIZE-$n$, which includes two main components:

(1) A **decision problem**, EXISTSECTORIZATION-$n(T)$, that determines the *existence* of a sectorization for node $n$ (with $K_n$, $\delta(n)$, and $\mathbf{f}_n$) under a given threshold value, $T \in \mathbb{R}_+$, given by

$$\text{EXISTSECTORIZATION-}n(T) = \begin{cases} (\text{Yes}, \nu_0), & \text{if } \exists \nu_0 \in \Gamma_n(K_n): \max\limits_{v\in\{n_1^{\nu_0},\cdots,n_{K_n}^{\nu_0}\}} \sum\limits_{e\in\delta(v)} f_e \le T, \\ (\text{No}, \varnothing), & \text{if } \forall \nu_0 \in \Gamma_n(K_n): \max\limits_{v\in\{n_1^{\nu_0},\cdots,n_{K_n}^{\nu_0}\}} \sum\limits_{e\in\delta(v)} f_e > T. \end{cases} \quad (15)$$

EXISTSECTORIZATION-$n(T)$ can be solved as follows. Consider the set of edges incident to node $n$, $\delta(n) = (e'_1, \cdots, e'_{|\delta(n)|})$. Without loss of generality, we assume that the first sectoring axis of node $n$ is placed between its first and last sectors, i.e., $(|e'_1, \cdots, e'_{|\delta(n)|})$. The second sectoring axis will be placed between the $k^{\text{th}}$ and $(k+1)^{\text{th}}$ incident edges if $\sum_{i=1}^{k} f_{e'_i} \le T$ and $\sum_{i=1}^{k+1} f_{e'_i} > T$.

Then, the process is repeated for the remaining edges $\delta(n) \setminus \{e_1, \cdots, e_k\}$ to find the third sectoring axis, so on and so forth until all edges in $\delta(n)$ are enumerated for the threshold, $T$.

(2) A **binary search process** that finds the critical threshold, $T_n^{\text{crit}}$, based on which the optimized sectorization for node $n$, denoted by $\pi_n$, is determined by EXISTSECTORIZATION-$n(T_n^{\text{crit}})$.

The following theorem states our main results regarding the correctness of SECTORIZE-$n$ and its guaranteed performances as a distributed approximation algorithm.

THEOREM 6.5. *For a given network flow* $\mathbf{f}$*, it holds that:*

*(i) [**Correctness**] The sectorization of node n returned by* SECTORIZE-n*,* $\pi_n(\mathbf{f}_n)$*, is equivalent to* $\nu_n(\mathbf{f}_n)$ *in (**Opt-Approx**-n), i.e.,*

$$\pi_n(\mathbf{f}_n) = \nu_n(\mathbf{f}_n),\ \forall n \in \mathcal{N}, \quad (16)$$

**Algorithm 2** EXISTSECTORIZATION-$n(T)$ for node $n$.

**Input**: $K_n$, $\delta(n)$, $\mathbf{f}_n$, and $T$
**for** $e \in \delta(n)$ **do**
  Reset node $n$'s sectorization $\pi_n \leftarrow \varnothing$
  Put a sectorizing axis in $\pi_n$ right after $e$ (clockwise)
  sectors_needed $\leftarrow 1$, total_weight $\leftarrow 0$
  $e' \leftarrow$ the edge next to $e$ in $\delta(n)$ (clockwise)
  **while** $e' \neq e$ **do**
    **if** $f_{e'} > T$ **then return** (NO, $\varnothing$)
    **else**
      total_weight $\leftarrow$ total_weight $+ f_{e'}$
      **if** total_weight $> T$ **then**
        sectors_needed $\leftarrow$ sectors_needed $+ 1$
        Put a sectorizing axis in $\pi_n$ before $e'$ (counter-clockwise)
        total_weight $\leftarrow f_{e'}$
      **end if**
      $e' \leftarrow$ the edge next to $e$ in $\delta(n)$ (clockwise)
    **end if**
  **end while**
  **if** sectors_needed $\le K_n$ **then**
    **return** (Yes, $\pi_n$)
  **end if**
**end for**
**return** (No, $\varnothing$)

*(ii) [**Approximation Ratio**] The distributed* SECTORIZE-n *algorithm is a* $2/3$*-approximation algorithm, i.e.,*

$$\tfrac{2}{3} \le \frac{\lambda^{\pi}(\mathbf{f})}{\lambda^{\sigma^\star}(\mathbf{f})} \le 1, \quad (17)$$

*where* $\lambda^{\sigma^\star}(\mathbf{f})$ *is flow extension ratio achieved by the optimal sectorization as the solution to (**Opt**).*

PROOF. *First, we prove (i).* We show that the decision returned by EXISTSECTORIZATION-$n(T)$ has a monotonic property with respect to $T$, i.e., there exists a *critical threshold*, $T_n^{\text{crit}} \in \mathbb{R}_+$, such that

$$\text{EXISTSECTORIZATION-}n(T) = \begin{cases} (\text{No}, \varnothing), & \forall T \in [0, T_n^{\text{crit}}), \\ (\text{Yes}, \cdot), & \forall T \in [T_n^{\text{crit}}, +\infty). \end{cases} \quad (18)$$

It is easy to see that EXISTSECTORIZATION-$n(T)$ outputs No for $T = 0$ and Yes for a sufficiently large $T$ with a non-zero flow $\mathbf{f}$. Let $T_n^{\text{crit}}$ be the smallest $T$ such that $\exists \pi_n \in \Gamma_n(K_n)$ with which the output of (15) is (Yes, $\pi_n$). As a result, we have EXISTSECTORIZATION-$n(T) =$ (No, $\varnothing$), $\forall T \in [0, T_n^{\text{crit}})$. In addition, $\pi_n$ and $T_n^{\text{crit}}$ satisfy

$$\max_{v\in\{n_1^{\pi_n},\cdots,n_{K_n}^{\pi_n}\}} \sum_{e\in\delta(v)} f_e \le T,\ \forall T \in [T_n^{\text{crit}}, +\infty).$$

Therefore, for a network flow $\mathbf{f}_n$ incident to node $n$, we can set

$$T_n^{\text{crit}} = \min_{\sigma_n\in\Gamma_n(K_n)} \Big\{ \max_{v\in\{n_1^{\sigma_n},\cdots,n_{K_n}^{\sigma_n}\}} \sum_{e\in\delta(v)} f_e \Big\}, \quad (19)$$

and the sectorization of node $n$ corresponding to $T_n^{\text{crit}}$ is equivalent to $\nu_n$ in (**Opt-Approx**-$n$), i.e.,

$$\pi_n(\mathbf{f}) = \arg\min_{\sigma_n\in\Gamma_n(K_n)} \Big\{ \max_{v\in\{n_1^{\sigma_n},\cdots,n_{K_n}^{\sigma_n}\}} \sum_{e\in\delta(v)} f_e \Big\} \overset{(13)}{=} \nu_n(\mathbf{f}_n). \quad (20)$$

Due to the monotonicity of (18), the critical value $T_n^{\text{crit}}$ can be found via a binary search within the interval $[\max_{e\in\delta(n)} f_e, \sum_{e\in\delta(n)} f_e]$ with a sufficiently small $\epsilon$, which is a parameter that controls the trade-offs between accuracy and convergence of Algorithm 1. Then, $\pi_n(\mathbf{f}_n)$ can be obtained via EXISTSECTORIZATION-$n(T_n^{\text{crit}})$.

*Next, we prove (ii).* For a network flow $\mathbf{f}$, consider the sectorizations $\sigma^\star(\mathbf{f})$ and $\widetilde{\sigma}(\mathbf{f})$ as the solution to (**Opt**) and (**Opt-Approx**), respectively. It is easy to see from their definitions that $\lambda^{\pi}(\mathbf{f}) \leq \lambda^{\sigma^\star}(\mathbf{f}) \Rightarrow \frac{\lambda^{\pi}(\mathbf{f})}{\lambda^{\sigma^\star}(\mathbf{f})} \leq 1$. From (11)–(12) and Lemma 5.3, we have

$$\lambda^{\sigma^\star}(\mathbf{f}) \leq \mu^{\sigma^\star}(\mathbf{f}) \leq \mu^{\widetilde{\sigma}}(\mathbf{f}) \text{ and } \tfrac{2}{3} \cdot \mu^{\widetilde{\sigma}}(\mathbf{f}) \leq \lambda^{\widetilde{\sigma}}(\mathbf{f}), \quad (21)$$

which further implies that

$$\tfrac{2}{3} \cdot \lambda^{\sigma^\star}(\mathbf{f}) \leq \tfrac{2}{3} \cdot \mu^{\widetilde{\sigma}}(\mathbf{f}) \leq \lambda^{\widetilde{\sigma}}(\mathbf{f}). \quad (22)$$

In addition, since $\pi(\mathbf{f}) = \nu(\mathbf{f}) = \widetilde{\sigma}(\mathbf{f})$ (see Theorem 6.5 (*i*) and Lemma 6.4), we can conclude that

$$\tfrac{2}{3} \cdot \lambda^{\sigma^\star}(\mathbf{f}) \leq \lambda^{\widetilde{\sigma}}(\mathbf{f}) = \lambda^{\pi}(\mathbf{f}) \Rightarrow \frac{\lambda^{\pi}(\mathbf{f})}{\lambda^{\sigma^\star}(\mathbf{f})} \geq \tfrac{2}{3}, \quad (23)$$

and Theorem 6.5 (*ii*) follows directly. □

Remark 6.1 (Complexity of Sectorize-*n*). *Recall from the proof of Theorem 6.5 that* $T_n^{crit} \in [\max_{e \in \delta(n)} f_e, \sum_{e \in \delta(n)} f_e]$. *Let* $\Theta := (\sum_{e \in \delta(n)} f_e - \max_{e \in \delta(n)} f_e)/\epsilon$, *the binary search process of Sectorize-n will terminate in* $O(\log_2 \Theta)$ *iterations, and each iteration has a complexity of* $O(|\delta(n)|^2)$ *(see Algorithm 2). Therefore, the complexity of Sectorize-n is* $O(|\delta(n)|^2 \cdot \log_2 \Theta) = O(N^2 \cdot \log_2 \Theta)$.

Remark 6.2. *Based on Lemma 5.3, we can obtain another lower bound of the approximation ratio of Sectorize-n given by:*

$$\frac{\lambda^{\pi}(\mathbf{f})}{\lambda^{\sigma^\star}(\mathbf{f})} \geq \frac{1}{1+\lambda^{\sigma^\star}(\mathbf{f}) \cdot \max_{e \in E^{\sigma}} f_e} \geq \frac{1}{1+\mu^{\pi}(\mathbf{f}) \cdot \max_{e \in E^{\sigma}} f_e} := LB^{\pi}(\mathbf{f}). \quad (24)$$

This bound is useful since, from the definition of $\lambda^{\sigma^\star}(\mathbf{f})$, i.e., the extension ratio of $\mathbf{f}$ for it "hit" the boundary of $\mathcal{P}_{H^{\sigma^\star}}$, the values of $\lambda^{\sigma^\star}(\mathbf{f})$ and $\max_{e \in E^{\sigma}} f_e$ can not be large simultaneously. Although $\lambda^{\sigma^\star}(\mathbf{f})$ is analytically intractable, since $\lambda^{\sigma^\star}(\mathbf{f}) \leq \mu^{\sigma^\star}(\mathbf{f}) \leq \mu^{\pi}(\mathbf{f})$, we can derive another lower bound of the approximation ratio, $LB^{\pi}(\mathbf{f})$, which depends on $\mu^{\pi}(\mathbf{f})$. Note that $LB^{\pi}(\mathbf{f})$ is tractable since $\max_{e \in E^{\sigma}} f_e$ is independent of the sectorization and $\mu^{\pi}(\mathbf{f})$ can be explicitly computed (10). In other words,

$$\max\left\{\tfrac{2}{3}, LB^{\pi}(\mathbf{f})\right\} \leq \frac{\lambda^{\pi}(\mathbf{f})}{\lambda^{\sigma^\star}(\mathbf{f})} \leq 1. \quad (25)$$

In §7.2, we show that for small values of $K_n$, $LB^{\pi}(\mathbf{f})$ is indeed a much tighter bound than 2/3 in (17).

**Discussions.** The distributed Sectorize-*n* algorithm approximates the optimal sectorization, $\sigma^\star(\mathbf{f})$, which maximizes the flow extension ratio, $\lambda^{\sigma}(\mathbf{f})$, under given $\mathbf{f}$ and $\mathbf{K} \in \mathbb{Z}_+^N$. Clearly, the choice of a sectorization should be based on a network flow, $\mathbf{f}$ as the polytope $\mathcal{P}_{H^{\sigma}}$ can be augmented in different flow directions depending on $\sigma$. Some discussions about the proposed optimization framework:

- *Dynamic Sectorization based on Backpressure.* With an (unknown and/or time-varying) arrival rate matrix $\boldsymbol{\alpha} \in \text{int}(\Lambda(G^{\sigma}))$ and a given sectorization $\sigma \in \Gamma(\mathbf{K})$, the dynamic backpressure algorithm will converge to and return a network flow $\mathbf{f} \in \mathcal{P}_{H^{\sigma}}$. Using the proposed framework, one can find the sectorization that approximates the best sectorization with respect to $\mathbf{f}$. The rationale behind this is that the sectorized network will be able to maintain arrival rates proportionally higher than $\boldsymbol{\alpha}$. Moreover, when $\lambda^{\widetilde{\sigma}}(\mathbf{f})$ is analytically tractable, it can provide information about how much $\mathbf{f}$ can be extended until it intersects with the boundary of the matching polytope $\mathcal{P}_{H^{\widetilde{\sigma}}}$. Therefore, the proposed framework can enable *dynamic sectorization* of the network to adapt to every network flow $\mathbf{f}$ obtained by the backpressure algorithm, including in scenarios with time-varying arrival rates, $\boldsymbol{\alpha}$.
- *Known Arrival Rates.* In the case with single-hop traffic, the capacity region of a network $G^{\sigma}$ is given by $\Lambda(G^{\sigma}) = \text{Co}(\mathcal{X}_{G^{\sigma}})$ (see (5)). With a known arrival rate matrix $\boldsymbol{\alpha}$, Sectorize-*n* augments the capacity region with respect to the required $\boldsymbol{\alpha}$. Similarly, in the case of multi-hop traffic, with a known $\boldsymbol{\alpha}$, one can first obtain a feasible multi-commodity network flow $\mathbf{f}$ that supports $\boldsymbol{\alpha}$, and then augment the polytope $\mathcal{P}_{H^{\sigma}}$ according to this $\mathbf{f}$.
- *Varying the Number of Sectors.* With proper (minor) modifications, Sectorize-*n* can also return the minimum number of sectors $K_n$ for every node $n$ such that a given network flow, $\mathbf{f}$, can be maintained by the network, i.e., $\mathbf{f} \in \mathcal{P}_{H^{\widetilde{\sigma}}}$. This is due to the distributed nature the proposed optimization framework, (**Opt-Approx**-*n*). Compared to previous work (e.g., [12]) whose objective is to obtain the minimum rate required for a network to support a flow vector $\mathbf{f}$, our proposed framework also provides a method to support $\mathbf{f}$ via efficient sectorization based on available resources.

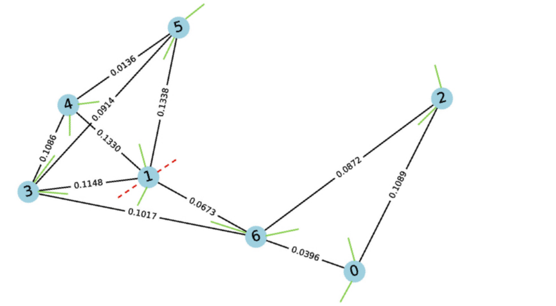


**Figure 6: An example 7-node network: the connectivity graph with the network flow f labeled on each edge. The green lines indicate the node sectorization, $\pi(\mathbf{f})$, obtained via Sectorize-*n* with $K_n = 2, \forall n$ with a sectorization gain of 1.83. The red dashed lines indicate a "misconfigured" sectorization of node 1 in the bottleneck phenomenon.**

# 7 EVALUATION

We now evaluate the sectorization gain and the performance of the distributed approximation algorithm via simulations. We focus on: (*i*) an example 7-node network, and (*ii*) random networks with varying number of nodes, number of sectors per node, and network flows. For each network and a given network flow, $\mathbf{f}$, we consider:

- $\pi_n(\mathbf{f}_n)$: the sectorization of node $n$ returned by the distributed approximation algorithm, Sectorize-*n* (Algorithm 1 in §6.2), and $\pi(\mathbf{f}) = (\pi_n(\mathbf{f}_n) : \forall n \in \mathcal{N})$ is the sectorization of all nodes.
- $\mu^{\pi}(\mathbf{f})$ and $\mu^{\varnothing}(\mathbf{f})$: the approximate flow extension ratios for the sectorized and unsectorized networks, respectively (§5).
- $g_{\mu}^{\pi}(\mathbf{f})$: the approximate sectorization gain achieved by $\pi(\mathbf{f})$ (§5).

## 7.1 An Example 7-node Network

We consider a 7-node network, whose connectivity graph is shown in Fig. 6, with a network flow $\mathbf{f}$ labeled on each edge and $\theta_{\text{th}} = 15.8°$ (see §3.2). For tractability and illustration purposes, we set $K_n = 2, \forall n$, and the green lines in Fig. 6 indicate the sectorization $\pi(\mathbf{f})$ returned by Sectorize-*n*. For this relatively small network, we can explicitly compute the flow extension ratios for both the sectorized network, $\lambda^{\pi}(\mathbf{f}) = \mu^{\pi}(\mathbf{f}) = 4.06$, and the unsectorized network,

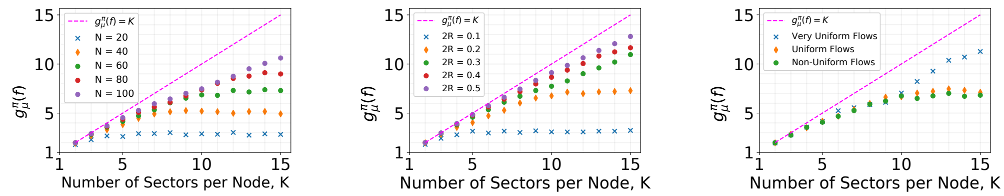

(a) (b) (c)

**Figure 7: The approximate sectorization gain, $g^{\pi}_{\mu}(\mathbf{f})$, as a function of the number of sectors per node, $K$, in random networks: (a) varying number of nodes $N \in \{20, 40, 60, 80, 100\}$ in networks with $2R = 0.2$ and *Uniform* flows, (b) varying communication range $2R \in \{0.1, 0.2, 0.3, 0.4, 0.5\}$ with *Uniform* flows and $N = 60$, and (c) varying network flows (*Non-uniform, Uniform, Very Uniform*) in networks with $N = 60$ and $2R = 0.2$.**

$\lambda^{\varnothing}(\mathbf{f}) = \mu^{\varnothing}(\mathbf{f}) = 2.22$. Therefore, the approximate sectorization gain $g^{\pi}_{\mu}(\mathbf{f})$ is equal to the explicit sectorization gain, i.e., $g^{\pi}_{\mu}(\mathbf{f}) = g^{\pi}_{\lambda}(\mathbf{f}) = 1.83$, which is close to $K_n = 2$.

Note that optimizing the sectorization of each node under a given $\mathbf{f}$ is critical, since the misplacement of the sectoring axes of even a single node can largely affect the achievable sectorization gain. We call this effect the *bottleneck phenomenon* in sectorized networks, as illustrated by the following example. Considered the optimized sectorization $\pi(\mathbf{f})$ shown by the green lines in Fig. 6. If only the sectorization of node 1 is "misconfigured" to be the red dashed lines, the sectorization gain is decreased from 1.83 to 1.22. This is also intuitive since with this misconfiguration, all three edges incident to node 1 with the highest flows are served by the same sector.

Since nodes 1, 3, and 6 in Fig. 6 have a maximum node degree of 4, we also obtain a sectorization $\pi(\mathbf{f})$ by running Sectorize-$n$ with $K_n = 4$. As expected, in the optimized sectorization for nodes 1, 3, and 6, one sectoring axis is put between every pair of adjacent edges. With this $\pi(\mathbf{f})$, we can also explicitly compute the flow extension ratios for the sectorized network $\lambda^{\pi}(\mathbf{f}) = \mu^{\pi}(\mathbf{f}) = 7.47$. With $\lambda^{\varnothing}(\mathbf{f}) = \mu^{\varnothing}(\mathbf{f}) = 2.22$, the sectorization gain is $g^{\pi}_{\mu}(\mathbf{f}) = g^{\pi}_{\lambda}(\mathbf{f}) = 3.36$. This example 7-node network demonstrates the performance and flexibility of Sectorize-$n$ for optimizing the deployment and configuration of sectorized networks based on the network flows.

## 7.2 Random Networks

We now consider networks with randomly generated connectivity graphs, $G$. In particular, for each generated random geometric graph, $N$ nodes are placed uniformly at random in a unit square area, and two nodes are joined by an edge if the distance between them is less than $2R$. We are interested in the effects of the following parameters of a random network on the sectorization gain:

- **Number of Nodes**, $N$: We consider random networks with different sizes of $N \in \{20, 40, 60, 80, 100\}$, and the network density increases with larger values of $N$.
- **Number of Sectors Per Node**, $K_n$: We assume all nodes have an equal number of sectors, $K_n = K, \forall n$, with $K \in \{2, 3, \ldots, 15\}$.
- **Communication Range**, $2R$: With a given number nodes, $N$, the connectivity of the network can be tuned by the communication range between two nodes, $2R$. We consider $2R \in \{0.1, 0.2, \ldots, 0.5\}$.
- **Uniformity of Network Flows**, $\phi$: For a network flow $\mathbf{f}$, we define its *uniformity* by $\phi := \max_e f_e / \min_e f_e$, i.e., $\mathbf{f}$ is more uniform if its $\phi$ is closer to 1. For a given value of $\phi$, random network flows $\mathbf{f}$ can be generated as follows. First, each element of $\mathbf{f}' = (f'_e)$ is independently drawn from a uniform distribution between $[1, \phi]$. Then, $\mathbf{f}$ is set to be $\mathbf{f}'$ after normalization, i.e., $\mathbf{f} = \mathbf{f}'/|\mathbf{f}|$. We consider *Non-uniform*, *Uniform*, and *Very Uniform* network flows with $\phi = 1000, 10,$ and $1.1$, respectively.

For random networks with a large number of nodes, we only consider $g^{\pi}_{\mu}(\mathbf{f})$ since it is computationally expensive to obtain $g^{\pi}_{\lambda}(\mathbf{f})$, which is the true sectorization gain achieved by $\pi(\mathbf{f})$. However, from Lemma 5.3, $g^{\pi}_{\mu}(\mathbf{f})$ provides good upper and lower bounds on $g^{\pi}_{\lambda}(\mathbf{f})$. The performance evaluation of each combination of these parameters is based on 1,000 instances of the random networks and their corresponding $\pi(\mathbf{f})$ obtained by Sectorize-$n$.

**Varying Number of Nodes,** $N$. Fig. 7(a) plots the approximate sectorization gain, $g^{\pi}_{\mu}(\mathbf{f})$, as a function of the number of sectors per node, $K$, in a network with $2R = 0.2$ and uniform flows ($\phi = 10$), with varying number of nodes, $N$. It can be observed that $g^{\pi}_{\mu}(\mathbf{f})$ increases sublinearly with respect to $K$, and it approaches the identity line of $g^{\pi}_{\mu}(\mathbf{f}) = K$ as $N$ increases, which is as expected. Note that with a practical value of $K$ (e.g., $K \leq 6$), these networks can achieve $g^{\pi}_{\mu}(\mathbf{f})$ that is almost equal to the number of sectors per node, $K$. In addition, as the value of $K$ increases, $g^{\pi}_{\mu}(\mathbf{f})$ deviates from $K$, which reveals a tradeoff point between the achievable sectorization gain ($g^{\pi}_{\mu}(\mathbf{f})$) and complexity of network deployments ($N$ and $K$). In fact, for given parameters $N$, $2R$, and $\phi$, i.e., for a given density of the network, there exists a number of sectors that saturates the gain $g^{\pi}_{\mu}(\mathbf{f})$. This can be explained by the fact that after a sufficiently large number of sectors, the auxiliary graph of the network breaks down to isolated pairs of nodes.

**Varying Communication Range,** $2R$. Fig. 7(b) plots the approximate sectorization gain, $g^{\pi}_{\mu}(\mathbf{f})$, as a function of the number of sectors per node, $K$, with $N = 60$, *Uniform* flows, $\phi = 10$, and varying communication ranges, $2R$. It can be observed that $g^{\pi}_{\mu}(\mathbf{f})$ increases sublinearly with respect to $K$. As expected, with the same number of nodes, $N = 60$, $g^{\pi}_{\mu}(\mathbf{f})$ is closer to $K$ as the range increases. In fact, there is a relationship between the parameters $N$ and $2R$: they both increase the number of neighbors for every node. The improved sectorization gains stem from the fact that since each node has a larger number of neighboring nodes (and thus links), a larger value of $K$ and the optimized sectorization can support a larger number of concurrent flows.

**Varying Uniformity of Network Flows,** $\phi$. Fig. 7(c) plots $g^{\pi}_{\mu}(\mathbf{f})$ as a function of the number of sectors per node, $K$, in a network with $N = 60$, $2R = 0.2$, and varying network flow uniformity (*Non-uniform*, *Uniform*, and *Very Uniform*). Overall, similar trends can be observed as those in Figs. 7(a) and 7(b). In general, more uniform network flows lead to improved values of $g^{\pi}_{\mu}(\mathbf{f})$, since non-uniform flows would have some larger flow components than the uniform

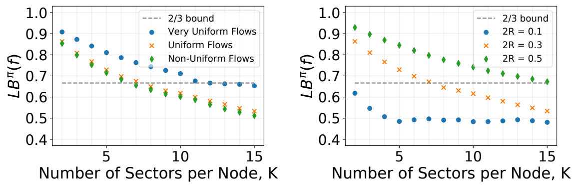


**Figure 8: The lower bound of approximation ratio of Sectorize-*n*, $LB^{\pi}(\mathbf{f})$ in (24), as a function of the number of sectors per node, $K$, with $N = 60$: (left) varying network flows in a network with $2R = 0.2$, and (right) varying communication ranges with *Uniform* flows.**

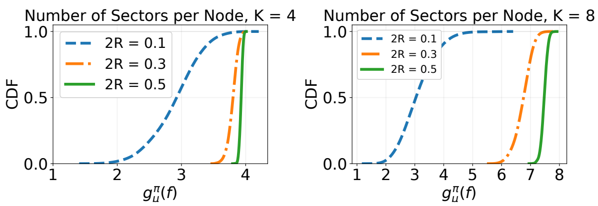


**Figure 9: The cumulative distribution function (CDF) of $g^{\pi}_{\mu}(\mathbf{f})$ with $N = 60$ and *Uniform* network flows.**

ones, which on average increases the value of $\mu^{\sigma}(\mathbf{f})$ (see (10)). In addition, recall the bottleneck phenomenon described in §7.1, it is more beneficial to divide the flows of a node more equally across its sectors to achieve an improved sectorization gain.

**Evaluation of the Lower Bound, $LB^{\pi}(\mathbf{f})$.** Using simulations, we also evaluate the lower bound of the approximation ratio of Sectorize-*n*, $LB^{\pi}(\mathbf{f})$ in (24), which depends on $\mu^{\tilde{\sigma}}(\mathbf{f})$ and $\mathbf{f}$. Fig. 8 plots the value of $LB^{\pi}(\mathbf{f})$ as a function of $K$ with varying uniformity of the network flows and node densities. It can be observed that for small values of $K$, $LB^{\pi}(\mathbf{f})$ is much higher than lower bound of 2/3 provided by Theorem 6.5. In particular, the difference between the bounds increases dramatically and the approximation becomes closer to the optimal for a small number of sectors. This is because in such networks, the maximum flow is expected to be small and hence $LB^{\pi}(\mathbf{f})$ can be improved when $\mu^{\tilde{\sigma}}(\mathbf{f})$ remains the same.

**CDF of the Approximate Sectorization Gain, $g^{\pi}_{\mu}(\mathbf{f})$.** Finally, we evaluate the relationship between $g^{\pi}_{\mu}(\mathbf{f})$ and the number of sectors, $K$. Fig. 9 plots the CDF of $g^{\pi}_{\mu}(\mathbf{f})$ with $N = 60$ and *Uniform* network flows with varying communication ranges. It can be seen that for networks with $2R = 0.3$, $g^{\pi}_{\mu}(\mathbf{f})$ has a median value of 3.7/6.5 for $K = 4/8$, respectively. This demonstrates the (sublinear) gain introduced by node sectorization, and this gain approaches the number of sectors per node, $K$, as the underlying is more connected.

## 8 CONCLUSION

In this paper, we considered wireless networks employing sectorized infrastructure nodes that form a multi-hop mesh network for data forwarding and routing. We presented a general sectorized node model and characterized the capacity region of these sectorized networks. We defined the flow extension ratio and sectorization gain of these networks, which quantitatively measure the performance gain introduced by node sectorization as a function of the network flow. We developed an efficient distributed algorithm that obtains the node sectorization with an approximation ratio of 2/3. We evaluated the proposed algorithm and the achieved sectorization gain in various network scenarios via extensive simulations.

## ACKNOWLEDGEMENTS

This work was supported in part by NSF grants CNS-2128530, CNS-2128638, CNS-2146838, CNS-2211944, AST-2232458, and by ARO MURI grant W911NF2110325.

## REFERENCES

[1] Mamta Agiwal, Abhishek Roy, and Navrati Saxena. 2016. Next generation 5G wireless networks: A comprehensive survey. *IEEE Commun. Surveys Tuts.* (2016).
[2] Edgar Arribas, Antonio Fernández Anta, Dariusz R Kowalski, Vincenzo Mancuso, Miguel A Mosteiro, Joerg Widmer, and Prudence WH Wong. 2019. Optimizing mmWave wireless backhaul scheduling. *IEEE Trans. Mobile Comput.* 19, 10 (2019).
[3] Tianyang Bai and Robert W Heath. 2014. Coverage and rate analysis for millimeter-wave cellular networks. *IEEE Trans. Wireless Commun.* 14, 2 (2014).
[4] Fei Dai and Jie Wu. 2006. Efficient broadcasting in ad hoc wireless networks using directional antennas. *IEEE Trans. Parallel Distrib. Syst.* 17, 4 (2006).
[5] Jack Edmonds. 1965. Maximum matching and a polyhedron with 0, 1-vertices. *J. Research of the National Bureau of Standards B* 69, 125-130 (1965), 55–56.
[6] Jack Edmonds. 1965. Paths, trees, and flowers. *Canadian J. Mathematics* (1965).
[7] Facebook. 2020. SuperCell: Reaching new heights for wider connectivity https://engineering.fb.com/2020/12/03/connectivity/supercell-reaching-new-heights-for-wider-connectivity.
[8] Juan García-Rois, Felipe Gomez-Cuba, et al. 2015. On the analysis of scheduling in dynamic duplex multihop mmWave cellular systems. *IEEE Trans. Wireless Commun.* 14, 11 (2015), 6028–6042.
[9] Marco Giordani, Michele Polese, et al. 2020. Toward 6G networks: Use cases and technologies. *IEEE Commun. Mag.* 58, 3 (2020).
[10] Manan Gupta, Anil Rao, Eugene Visotsky, Amitava Ghosh, and Jeffrey G Andrews. 2020. Learning link schedules in self-backhauled millimeter-wave cellular networks. *IEEE Trans. Wireless Commun.* 19, 12 (2020), 8024–8038.
[11] Piyush Gupta and Panganmala R Kumar. 2000. The capacity of wireless networks. *IEEE Trans. Inf. Theory* 46, 2 (2000), 388–404.
[12] Bruce Hajek and Galen Sasaki. 1988. Link scheduling in polynomial time. *IEEE Trans. Inf. Theory* 34, 5 (1988), 910–917.
[13] IEEE Spectrum. 2019. Facebook's 60-GHz Terragraph Technology. https://spectrum.ieee.org/facebooks-60ghz-terragraph-technology-moves-from-trials-to-commercial-gear#toggle-gdpr.
[14] Jeff Kahn. 1996. Asymptotics of the chromatic index for multigraphs. *Journal of Combinatorial Theory, Series B* 68, 2 (1996), 233–254.
[15] Thanasis Korakis, Gentian Jakllari, and Leandros Tassiulas. 2003. A MAC protocol for full exploitation of directional antennas in ad-hoc wireless networks. In *Proc. ACM MobiHoc'03.*
[16] Michele Polese, Marco Giordani, Tommaso Zugno, Arnab Roy, Sanjay Goyal, Douglas Castor, and Michele Zorzi. 2020. Integrated access and backhaul in 5G mmWave networks: Potential and challenges. *IEEE Commun. Mag.* 58, 3 (2020).
[17] Panagiotis Promponas, Tingjun Chen, and Leandros Tassiulas. 2023. Optimizing Sectorized Wireless Networks: Model, Analysis, and Algorithm. arXiv:2308.10970 [cs.NI]
[18] Theodore S Rappaport, Shu Sun, et al. 2013. Millimeter wave mobile communications for 5G cellular: It will work! *IEEE Access* 1 (2013), 335–349.
[19] Siuli Roy, Dola Saha, Somprakash Bandyopadhyay, Tetsuro Ueda, and Shinsuke Tanaka. 2003. A network-aware MAC and routing protocol for effective load balancing in ad hoc wireless networks with directional antenna. In *Proceedings of the 4th ACM international symposium on Mobile ad hoc networking & computing.*
[20] Bodhisatwa Sadhu, Yahya Tousi, et al. 2017. A 28-GHz 32-element TRX phased-array IC with concurrent dual-polarized operation and orthogonal phase and gain control for 5G communications. *IEEE J. Solid-State Circuits* 52 (2017).
[21] Alexander Schrijver et al. 2003. *Combinatorial optimization: Polyhedra and efficiency.* Vol. 24. Springer.
[22] Clayton Shepard, Hang Yu, Narendra Anand, Erran Li, Thomas Marzetta, Richard Yang, and Lin Zhong. 2012. Argos: Practical many-antenna base stations. In *Proc. ACM MobiCom'12.*
[23] Leandros Tassiulas and Anthony Ephremides. 1990. Stability properties of constrained queueing systems and scheduling policies for maximum throughput in multihop radio networks. In *Proc. IEEE CDC'90.*
[24] Zuoming Yu, Jin Teng, Xiaole Bai, Dong Xuan, and Weijia Jia. 2014. Connected coverage in wireless networks with directional antennas. *ACM Trans. Sens. Netw.* 10, 3 (2014).
[25] Dingwen Yuan, Hsuan-Yin Lin, Jörg Widmer, and Matthias Hollick. 2020. Optimal and approximation algorithms for joint routing and scheduling in millimeter-wave cellular networks. *IEEE/ACM Trans, Netw.* 28, 5 (2020), 2188–2202.
[26] Ding Zhang, Mihir Garude, and Parth H Pathak. 2018. mmChoir: Exploiting joint transmissions for reliable 60 GHz mmWave WLANs. In *Proc. ACM MobiHoc'18.*
[27] Guanglin Zhang, Youyun Xu, Xinbing Wang, and Mohsen Guizani. 2010. Capacity of hybrid wireless networks with directional antenna and delay constraint. *IEEE Trans. Commun.* 58, 7 (2010).